UNIVERSITY OF BIRMINGHAM
University of Birmingham Research at Birmingham

Path-planning of a hybrid parallel robot using stiffness and workspace for foot rehabilitation

Rastegarpanah, Alireza; Rakhodaei, Hamid; Saadat, Mozafar; Rastegarpanah, Mohammad; Marturi, Naresh; Borboni, Alberto; Loureiro, Rui C.V.

DOI:
10.1177/1687814017754159

License:
Creative Commons: Attribution (CC BY)

Document Version
Publisher's PDF, also known as Version of record

Citation for published version (Harvard):
Rastegarpanah, A, Rakhodaei, H, Saadat, M, Rastegarpanah, M, Marturi, N, Borboni, A & Loureiro, RCV 2018, 'Path-planning of a hybrid parallel robot using stiffness and workspace for foot rehabilitation', *Advances in Mechanical Engineering*, vol. 10, no. 1, pp. 1-10. https://doi.org/10.1177/1687814017754159

Link to publication on Research at Birmingham portal

General rights
Unless a licence is specified above, all rights (including copyright and moral rights) in this document are retained by the authors and/or the copyright holders. The express permission of the copyright holder must be obtained for any use of this material other than for purposes permitted by law.

•Users may freely distribute the URL that is used to identify this publication.
•Users may download and/or print one copy of the publication from the University of Birmingham research portal for the purpose of private study or non-commercial research.
•User may use extracts from the document in line with the concept of 'fair dealing' under the Copyright, Designs and Patents Act 1988 (?)
•Users may not further distribute the material nor use it for the purposes of commercial gain.

Where a licence is displayed above, please note the terms and conditions of the licence govern your use of this document.

When citing, please reference the published version.

Take down policy
While the University of Birmingham exercises care and attention in making items available there are rare occasions when an item has been uploaded in error or has been deemed to be commercially or otherwise sensitive.

If you believe that this is the case for this document, please contact UBIRA@lists.bham.ac.uk providing details and we will remove access to the work immediately and investigate.

Download date: 25. Apr. 2024

Check for updates

Special Issue Article

Advances in Mechanical Engineering

Advances in Mechanical Engineering
2018, Vol. 10(1) 1–10
© The Author(s) 2018
DOI: 10.1177/1687814017754159
journals.sagepub.com/home/ade
SAGE

Path-planning of a hybrid parallel robot using stiffness and workspace for foot rehabilitation

Alireza Rastegarpanah[1], Hamid Rakhodaei[2], Mozafar Saadat[2], Mohammad Rastegarpanah[3], Naresh Marturi[4], Alberto Borboni[5] and Rui CV Loureiro[1]

Abstract

Stiffness is one of the important parameters for estimating the performance of hybrid parallel robots as it is not constant throughout its workspace. The aim of this study is to provide an optimum path based on maximum stiffness within the workspace of a 9-degree-of-freedom hybrid parallel mechanism configuration, which includes nine linear actuators connecting one stationary and two moving platforms in series. The proposed robot is designed for ankle rehabilitation, where accurate and precise movement of lower extremities is required. The design takes advantage of two important characteristics of parallel robots: stiffness and workspace. The proposed methodology to determine the stiffness of hybrid robot in three single axes is based on calculation of position vector of each actuator in any particular pose, by considering the inverse kinematics of the system, in order to obtain the magnitude and direction of the applied forces. The results obtained from the workspace calculations have been compared with those of two standard parallel mechanisms including a 6-degree-of-freedom hexapod and a tripod with 3 degrees of freedom. The stiffness of the robot has been calculated in simulation and then compared with those of a developed prototype hybrid model in two different case studies.

Keywords

Stiffness, parallel robot, ankle rehabilitation, workspace, gait

Date received: 31 July 2017; accepted: 21 December 2017

Handling Editor: Tadeusz Mikolajczyk

Introduction

Stiffness and accuracy are the most important characteristics making parallel mechanisms suitable for applications such as medical operations, human–systems interaction, haptic interfaces and rehabilitation applications. Due to good size/power ratio and compact size, parallel robots are more appropriate than serial robots. Delta and hexapod are the most well-known structures of parallel robots with their kinematics and dynamics studied for decades. Usually, the stiffness of a tripod and a hexapod is determined by calculating the deformation caused by external force on the end-effector. Therefore, stiffness analysis of a parallel robot depends

[1]Centre for Rehabilitation Engineering and Assistive Technology, Institute of Orthopaedics and Musculoskeletal Sciences, University College London, London, UK
[2]School of Engineering, University of Birmingham, Birmingham, UK
[3]Faculty of Engineering, Najafabad Branch, Islamic Azad University, Najafabad, Iran
[4]KUKA Robotics UK Ltd, Wednesbury, UK
[5]Department of Mechanical and Industrial Engineering, University of Brescia, Brescia, Italy

Corresponding author:
Alireza Rastegarpanah, Centre for Rehabilitation Engineering and Assistive Technology, Institute of Orthopaedics and Musculoskeletal Sciences, University College London, London WC1E 6BT, UK.
Email: a.rastegarpanah@ucl.ac.uk

Creative Commons CC BY: This article is distributed under the terms of the Creative Commons Attribution 4.0 License (http://www.creativecommons.org/licenses/by/4.0/) which permits any use, reproduction and distribution of the work without further permission provided the original work is attributed as specified on the SAGE and Open Access pages (https://us.sagepub.com/en-us/nam/open-access-at-sage).

on the material properties and length of the actuators used.[1] In another study, the stiffness analysis of a parallel robot was determined by different parameters such as joints positions, structural architecture and end-effectors position.[2] Different researchers have calculated the stiffness of parallel robots based on a developed Jacobean matrix for different configurations.[3,4] Inverse kinematics (IK) has been used in different studies to find the workspace of the parallel mechanism.[5,6] Dimensional synthesis of a 3UPS-PRU parallel robot was investigated in order to reach maximum linear and angular velocity in desired workspace.[7]

The robust finite-time tracking of a Stewart platform using forward kinematic solution has been developed to determine the unique length for the actuators by considering all the uncertainties and parameter variations.[8] The stiffness of a six-legged platform was studied by Li et al.,[9] and calculated using IK and then compared with the results of finite element analysis (FEA). Zhang et al.,[10] and Masouleh et al.,[11] investigated combinational parallel mechanisms where their kinematics and dynamics calculated based on the kinematic change in the models. Due to the limited workspace of parallel robots, a new configuration (PARASURG-9M) was developed and its IK was investigated for surgery applications.[12] The hybrid or planner 3-degree-of freedom (DoF) parallel manipulator is a relatively new configuration of parallel robot which is developed to improve the limited workspace of a 6DoF parallel configuration.[13,14] This made the hybrid parallel robot more efficient to use for ankle rehabilitation.[15] 6DoF is needed in order to simulate the motion of the foot, but singularity and limited flexibility of the hexapod motivated us to push an idea for a new serial–parallel manipulator. The hybrid configuration is an elegant solution to increase the flexibility of the parallel robot and to achieve full range of foot motions. Hu et al.,[16] studied the stiffness of various configurations of hybrid parallel robots for elastic deformation. Zhao et al.,[17] developed a new formulation set up of stiffness for hybrid parallel kinematic mechanism (HPKM) in a multi-dimensional vibration isolator based on the screw theory method and the stiffness was evaluated considering compliances in different directions and the extremum values in the workspace.

Stiffness is one of the important parameters in estimating the performance of the hybrid parallel robots, particularly when the system is used as a rehabilitation device. The aim of this article is to calculate the stiffness and elastic deformation of 6-UPS-3SPR hybrid parallel robot. This article investigates the stiffness of a flexible configuration of a parallel robot by calculating the position vector of each actuator in the determined workspace of the system. This is carried out by calculating the stiffness matrix of the system. In the mathematical method, the workspace and stiffness of the tripod and the hexapod are calculated separately, and the data were combined together in order to determine the workspace and stiffness of the hybrid parallel robot. The external force applied by the foot was measured in the gait lab and the results were used in FEA. The final position and orientation of the end-effector are input data to the IK formulation in order to calculate the length of actuators. The developed formulation is based on a transformation matrix containing the rotational matrix with Euler angles and translation motion. The data are supported by experimental results tested on a robot prototype.

Methodology

Gait analysis

Fourteen participants including seven males (43 ± 5 years, 85 ± 3 kg) and seven females (44 ± 3 years, 63 ± 4 kg) signed the consent form in order to participate in our experiment which was performed in the gait laboratory of West Midlands Rehabilitation Centre (WMRC). As Figure 1 demonstrates, participants were asked to move their foot in dorsiflexion and plantar flexion directions in sitting position. The laboratory was equipped with 16 Vicon cameras (with frequency of 100 Hz) and 2 Kistler force plates (with a sampling frequency of 2000 Hz). In the sitting position, both right leg and left leg were placed on the force plate number 2 and number 1, respectively. Each participant had six trials in overall: three trials with the right leg and three trials with the left leg. The foot was moved in dorsiflexion direction first and then it moved in plantar flexion direction.

The captured data were processed using Vicon nexus 1.7.1, and a three-dimensional (3D) model of lower limb and profile of force were modelled. The position of the attached markers and the recorded data by the force plates were exported to MATLAB software to be filtered and normalised. A foot plane was defined by the attached markers 1, 2 and 3 that they were placed on ankle, toe and heel, respectively. By calculating the normal vector of the foot plane, the path motion of the foot was determined during ankle dorsiflexion/plantar flexion. Calculation of the normal vector of the foot segment has been explained in our previous work.[18]

Kinematic mapping motion

Generally, the position of a point can be identified by a transformation matrix containing six independent quantities (linear and rotational motions in XYZ). The homogeneous transformation matrix was used to calculate the position of the end-effector along the foot trajectory. The system contains two moving platforms, as shown in Figure 2.

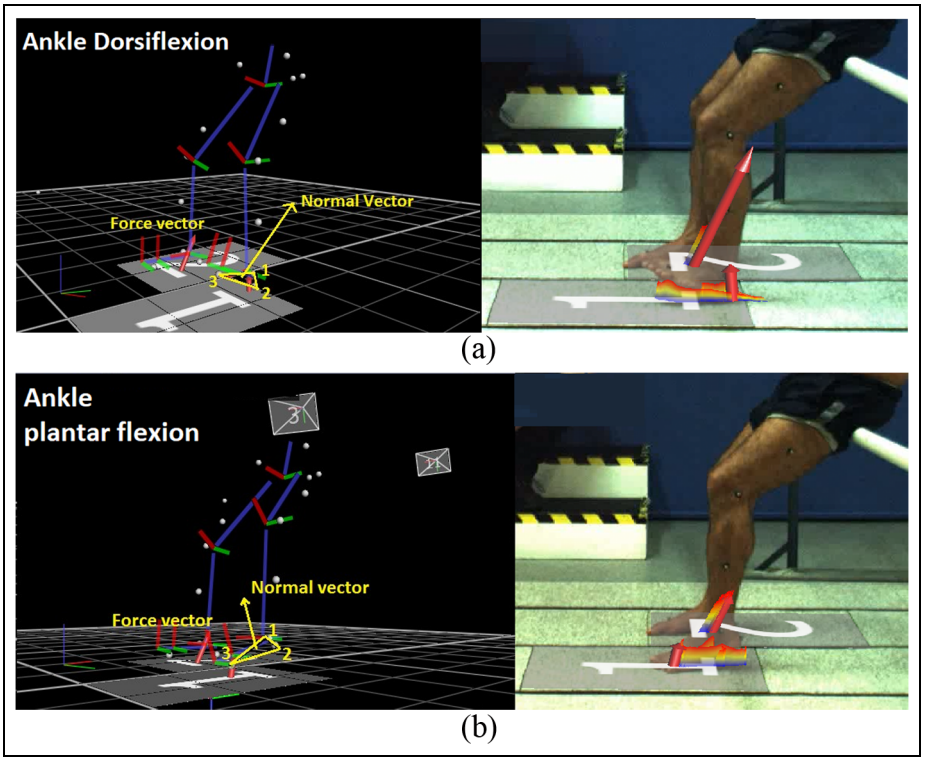

Figure 1. Simulated lower limb model of a participant during moving the left foot in (a) dorsiflexion and (b) plantar flexion directions. In the right side of both pictures, the Butterfly force profile is overlaid with the participant's foot. In the both pictures, force plates are labelled with numbers 1 and 2 in white colours.

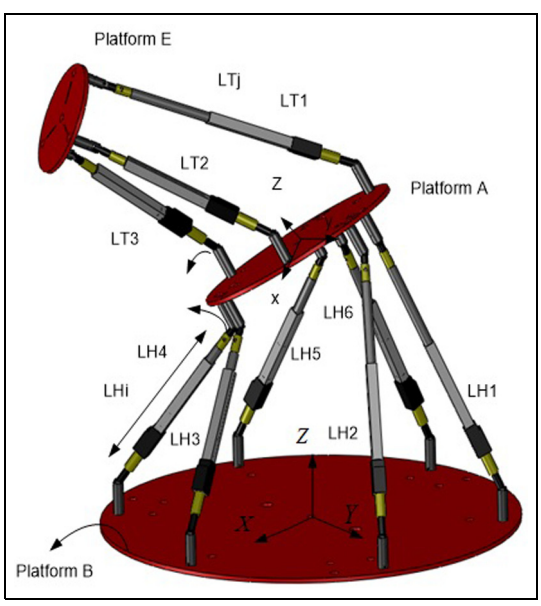

Figure 2. 3D CAD model of 9DoF parallel robot designed in SolidWorks. The global coordinate reference of the hybrid robot is placed on the centre of platform B.

The position vector of the actuators has been calculated using a developed kinematic and transformation matrix. The stroke length of actuators is important in order to find out the velocity of the actuators. Equations (1a) and (1b) calculate the actuators vector position

$$\mathbf{L}_{Hi} = \mathbf{A}_i T_B^A - \mathbf{B}_i \qquad i \in \{1 \ldots 6\} \tag{1a}$$

$$\mathbf{L}_{Tj} = \mathbf{E}_j T_E^A T_A^B - \mathbf{A}_i \quad j \in \{1 \ldots 3\},\ i \in \{7 \ldots 9\} \tag{1b}$$

where $\mathbf{L}_{Hi}$ represents the position vector of each actuator; T_B^A is the motion matrix of platform A with respect to platform B; $\mathbf{A}_i$ is the initial position of the joint on platform A and $\mathbf{B}_i$ is the position of the joints on platform B, while $\mathbf{E}_j$ is the initial position of the joints and T_A^E is the motion of platform E with respect to platform A. Moreover, $\mathbf{L}_{Tj}$ represents the position vectors of the actuators that connect platforms A and E.

Workspace analysis

IK identifies the positions of the platforms and the joints along the captured foot trajectory. However, applying the structural constraints of the design identifies the reachable points existing in the workspace. The stroke size and joints range of motion are the constraints considered in this study. The position of the joints on the hexapod for the motion of the ankle during dorsiflexion/plantar flexion is obtained by

equations (1a) and (1b). The system contains 18 joints, and the corresponding range of motion should be determined to calculate and analyse the workspace. The angles between the actuators and joints demonstrate the motion of the joints. The angles of the joints on platform B are calculated using equations (2a) and (2b)

$$\alpha_{Bi} = \cos^{-1}\left(\frac{U_x \cdot L_{Hi}}{|L_{Hi}|}\right) \quad i \in \{1 \ldots 6\} \tag{2a}$$

$$\beta_{Bi} = \cos^{-1}\left(\frac{U_y \cdot L_{Hi}}{|L_{Hi}|}\right) \quad i \in \{1 \ldots 6\} \tag{2b}$$

where U_x and U_y are axes of the joints on platform B; L_{Hi} is the actuator position vector; α_{Bi} is the angle of the joint with its X-axis and β_{Bi} is the angle of the joint with its Y-axis. The joints axes on platform A move with the motion provided for the system. The angles of the joint are calculated by equations (3a) and (3b)

$$\alpha_{Ai} = \cos^{-1}\left(\frac{u_x \cdot L_{Tj}}{|L_{Tj}|}\right) i \in \{1 \ldots 6\},\ j \in \{1 \ldots 3\} \tag{3a}$$

$$\beta_{Ai} = \cos^{-1}\left(\frac{u_y \cdot L_{Tj}}{|L_{Tj}|}\right) \quad i \in \{1 \ldots 6\},\ j \in \{1 \ldots 3\} \tag{3b}$$

where α_{Ai} and β_{Ai} are the joints angles with their own X-axis and Y-axis, respectively, and u_x and u_y are axes of the joints after the motion. u_x and u_y are changed with respect to U_x and U_y based on the rotational motions that applied to the system. Therefore, the axis of revolute joint on platform E is obtained by replacing u_x in equation (3b). However, the angles of revolute joints are obtained by (4)

$$\alpha_{Ej} = \cos^{-1}\left(\frac{u_{2x} \cdot L_{Tj}}{|L_{Tj}|}\right) \quad j \in \{1 \ldots 3\} \tag{4}$$

where α_{Ej} with $(j = 1, 2, 3)$ are the angles of the joints connecting to platform E after motion of the ankle in the defined rehabilitation exercise and u_{2x} is the axis of the revolute joint in a particular pose and orientation. The structural constraints are applied to the inputs of the desired motions. The workspace of the system was programmed with Cartesian and polar algorithms in MATLAB software packages. The initial positions are obtained using the data from the computer-aided design (CAD) model. The developed program calculates the workspace of the hexapod and tripod as well as that of the hybrid system during foot motion. The maximum stroke size of hybrid actuators is 100 mm while the length of the actuators in hexapod and tripod is 200 mm. The boundary 3D models of the tripod, hexapod and hybrid parallel robot are demonstrated in Figure 3(a)–(c) respectively.

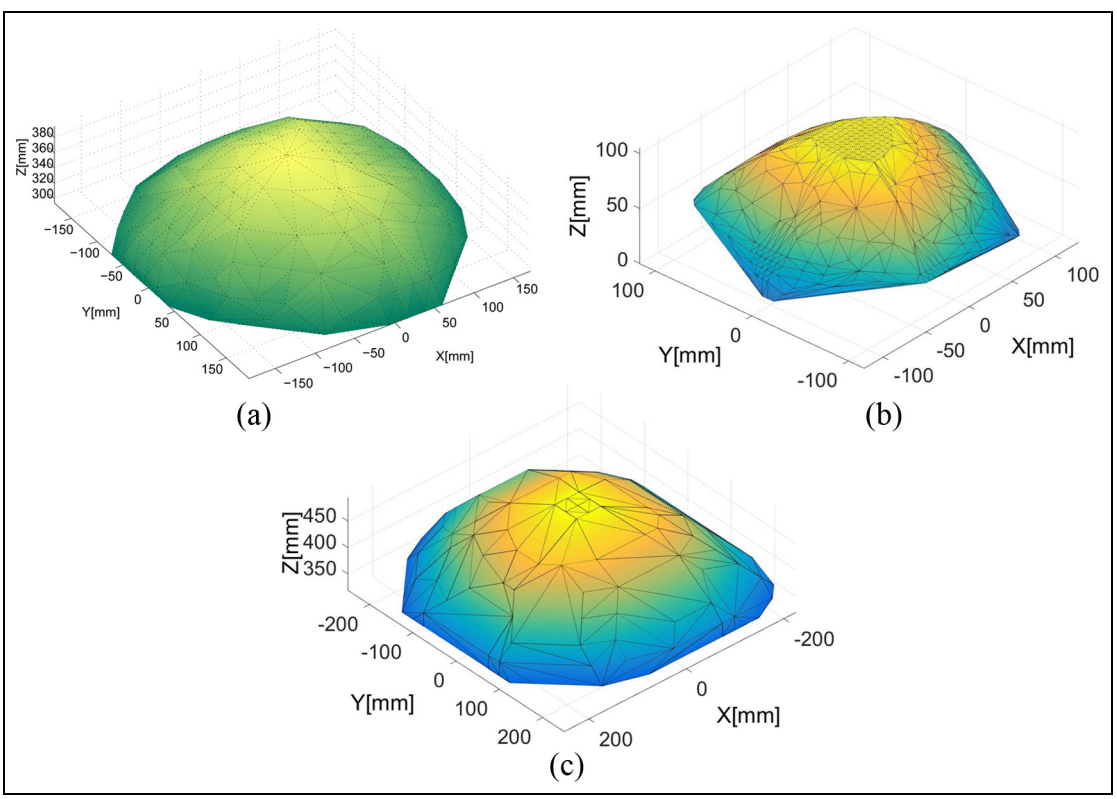

Figure 3. Simulated workspace of the three parallel configurations: (a) workspace of the 3-UPR tripod, (b) workspace of the 6DoF hexapod and (c) workspace of the 9DoF hybrid.

The results are based on the number of points assumed to be in the workspace; the shape of the workspace is more accurate by increasing the number of mesh nodes. The results produced by the numerical method, developed in MATLAB, suggested that the workspace of the hybrid robot is increased by 160% compared to that of the hexapod.

Stiffness analysis

In the Cartesian space (global frame), the pose X of the end-effector is determined by the position variables (x y z) and orientation variables (θ ϕ Ψ), as can be expressed by equation (5)[19]

$$X = [x\ y\ z\ \theta\ \phi\ \Psi]^{\mathrm{T}} \tag{5}$$

The exerted force on platform A is developed by (6)

$$F_{in}X = [F_1\ F_2\ F_3\ F_4\ F_5\ F_6]^{\mathrm{T}} \tag{6}$$

where F_{in} is the force matrix of hexapod created by actuators on platform A and actuator force F_i. In order to calculate the force vector, unit vector of actuators is calculated as follows

$$\mathbf{S}_i = \frac{\mathbf{L}_{Hi}}{\| L_{Hi} \|} \quad i \in \{1 \ldots 6\} \tag{7a}$$

$$\mathbf{F}_H = \sum_{i=1}^{6} \mathbf{s}_i F_i \tag{7b}$$

where $\mathbf{S}_i$ is the unit position vector of actuators, $\mathbf{L}_{Hi}$ is position vector of actuators and $\mathbf{F}_H$ is force applied to platform A. The created momentum on platform A due to linear forces of actuators is calculated by equation (8)

$$\mathbf{T_H} = \sum_{i=1}^{6} (\mathbf{A}_i \times s_i) F_i \tag{8}$$

The actuator force during the foot trajectory has been defined in a matrix format which is expressed in equation (9). Where $\mathbf{F_H}$ is the linear force and $\mathbf{T_H}$ is the torque generated by actuators. However, equation (9) is calculated by equation (8) and the force transformation matrix is

$$F_{out}(X) = [\mathbf{F_H}\ \ \mathbf{T_H}]^{\mathrm{T}} \tag{9}$$

The relation between input and output loads of the hexapod parallel manipulator is given by equation (10)

$$F_{out}(X) = H(X) F_{in}(X) \tag{10}$$

$H(X)$ is a 6×6 force transformation matrix which indicates how the output load is related to the input forces. The force transformation matrix of the base hexapod is obtained by equation (11). The force transformation matrix H represents the relations between the input forces F_{in} and the output forces F_{out}. The following model for calculating the applied force on the end-effector is demonstrated by $[F\ \ T]$, while F is the linear force and T is applied torque on the platform. The force diagram of upper 3-UPR is demonstrated in Figure 4.

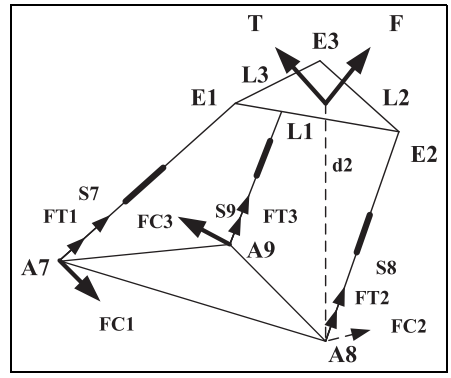

Figure 4. Free body diagram of applied forces on the 3-UPR configuration.

As it is expressed in equations (12a) and (12b), the applied force and torque on the platform are balanced by three active actuator forces which are expressed by FT_i, $(i = 1, 2, 3)$ and three constrained forces which are represented by FC_i, $i = (1, 2, 3)$. Each FT_i forces is alongside of the actuators and each FC_i forces is perpendicular to the actuators[20]

$$H(X) = \begin{bmatrix} \mathbf{s_1} & \mathbf{s_2} & \mathbf{s_3} & \mathbf{s_4} & \mathbf{s_5} & \mathbf{s_6} \\ \mathbf{A_1} \times \mathbf{s_1} & \mathbf{A_2} \times \mathbf{s_2} & \mathbf{A_3} \times \mathbf{s_3} & \mathbf{A_4} \times \mathbf{s_4} & \mathbf{A_5} \times \mathbf{s_5} & \mathbf{A_6} \times \mathbf{s_6} \end{bmatrix} \tag{11}$$

$$\begin{bmatrix} FT_1 \\ FT_2 \\ FT_3 \\ FC_1 \\ FC_2 \\ FC_3 \end{bmatrix} = -\left(J^{\mathrm{T}}\right)^{-1} R^{O}_{\theta\phi\Psi} \begin{bmatrix} F \\ T \end{bmatrix} \tag{12a}$$

$$J = \begin{bmatrix} \mathbf{S}_7^{\mathrm{T}} & (\mathbf{e}_1 \times \mathbf{S}_7)^{\mathrm{T}} \\ \mathbf{S}_8^{\mathrm{T}} & (\mathbf{e}_2 \times \mathbf{S}_8)^{\mathrm{T}} \\ \mathbf{S}_9^{\mathrm{T}} & (\mathbf{e}_3 \times \mathbf{S}_9)^{\mathrm{T}} \\ \mathbf{C}_1^{\mathrm{T}} & (\mathbf{d}_1 \times \mathbf{C}_1)^{\mathrm{T}} \\ \mathbf{C}_2^{\mathrm{T}} & (\mathbf{d}_2 \times \mathbf{C}_2)^{\mathrm{T}} \\ \mathbf{C}_3^{\mathrm{T}} & (\mathbf{d}_3 \times \mathbf{C}_3)^{\mathrm{T}} \end{bmatrix}_{6 \times 6} \tag{12b}$$

where c_i is the unit vector of Fc_i and $R^{O}_{\theta\phi\Psi}$ is rotation matrix of platform A. With regard to the principle of virtual work, despite the deformation in the system, the static balance is kept under all the applied forces.

Therefore, the sum of the work, which is generated by the external forces and the works generated by the internal forces along the deformation, must be zero. In the following equations, dx, dy and dz are three translation dimensions due to elastic deformation on the centre point of platform E, while $d\theta$, $d\phi$ and $d\psi$ are three rotational components due to elastic deformation on platform E. The stiffness matrix of the based platform has been calculated using equation (13).[20] The virtual work of the hexapods actuator plus that of the tripod would be equal to the virtual work on the end-effector as formulated in equation (18)

$$\begin{bmatrix} dr_1 \\ dr_2 \\ dr_3 \\ dr_4 \\ dr_5 \\ dr_6 \end{bmatrix}^{\mathrm{T}} \begin{bmatrix} F_1 \\ F_2 \\ F_3 \\ F_4 \\ F_5 \\ F_6 \end{bmatrix} + \begin{bmatrix} dr_{T1} \\ dr_{T2} \\ dr_{T3} \\ dc_1 \\ dc_2 \\ dc_3 \end{bmatrix}^{\mathrm{T}} \begin{bmatrix} FT_1 \\ FT_2 \\ FT_3 \\ FC_1 \\ FC_2 \\ FC_3 \end{bmatrix} = - \begin{bmatrix} dx \\ dy \\ dz \\ d\theta \\ d\phi \\ d\psi \end{bmatrix}^{\mathrm{T}} [\mathbf{F} \;\; \mathbf{T}]^{\mathrm{T}} \tag{13a}$$

$$\begin{bmatrix} dr_1 \\ dr_2 \\ dr_3 \\ dr_4 \\ dr_5 \\ dr_6 \end{bmatrix}^{\mathrm{T}} H(X)^{-1} + \begin{bmatrix} dr_{T1} \\ dr_{T2} \\ dr_{T3} \\ dc_1 \\ dc_2 \\ dc_3 \end{bmatrix}^{\mathrm{T}} \left(J^T\right)^{-1} R^{O}_{\theta\phi\Psi} G = \begin{bmatrix} dx \\ dy \\ dz \\ d\theta \\ d\phi \\ d\psi \end{bmatrix}^{\mathrm{T}} \tag{13b}$$

$$\begin{bmatrix} dx \\ dy \\ dz \\ d\theta \\ d\phi \\ d\psi \end{bmatrix} = \mathbf{C}[\mathbf{F} \;\; \mathbf{T}]^{\mathrm{T}}, \; [\mathbf{F} \;\; \mathbf{T}]^{\mathrm{T}} = K \begin{bmatrix} dx \\ dy \\ dz \\ d\theta \\ d\phi \\ d\psi \end{bmatrix} \tag{13c}$$

$$K = C^{-1} \tag{13d}$$

Results and discussion

Finite element analysis

In this section, the displacement of the hybrid parallel robot under applied force has been simulated in SolidWorks software and the results were used to validate the theoretical method. Foot trajectory and corresponding applied force, during dorsiflexion and plantar flexion movements, were recorded by the motion capture system and the force plates in the gait lab. The recorded position and force were averaged over all participant's trials. The results obtained for the left leg have been demonstrated in Figure 5(a) and (b). The gait results were used by the Motion Analysis toolbox in SolidWorks and the stiffness of the modelled hybrid robot was analysed while the model tracked the foot trajectories.

As shown in Figure 5(a), the maximum applied forces (Fx, Fy, Fz) during dorsiflexion and plantar flexion were (8.12 N, 1.46 N), (17.15 N, 1.28 N), (69.48 N, 36.57 N), respectively. With respect to the calculated deformation of the CAD model under load, the stiffness of the hybrid parallel robot is calculated in SolidWorks during tracking the foot motion. As it is shown in Figure 6(a), the deformation of components has been calculated separately in three axes of X, Y and Z. The solid mesh type with curvature base and four Jacobian points with the mesh size of 0.3 mm were used in the FEA. The element size and tolerance were 0.497 and 0.024 mm, respectively. In addition to the material properties of the actuators and joints, other mechanical properties of the robot have been considered in the simulation, such as physical structure, position and orientation of the end-effector. Based on the hypothesis of this study, the centre point of the foot is placed on the centre point of platform E. The $GRF_{X,Y,Z}$ applied on platform E, while the end-effector tracked the foot motion. Length of actuators was calculated by solving the IK mapping of the robot and the results were used by the developed CAD model in order to move the end-effector along the foot motion. With respect to the calculated deformation in time, the translational stiffness of the hybrid robot is calculated and shown in Figure 6(b).

By starting the dorsiflexion movement, the force profile has been shifted from the calcaneum towards the toes. The maximum deformation has been observed when the foot is in neutral position. Figure 6(b) shows that stiffness in the Z-axis has been sharply decreased once dorsiflexion motion completed and it has been reached to its minimum at 24 kN/mm when the heel was removed from the floor, and the calcaneum reached its maximum height from the floor.

A prototype of the hybrid robot was modelled and built in order to validate the simulation results. In the following section, the stiffness of the robot prototype is investigated during execution of different motions.

Experimentation validations

A hybrid robot was built using nine servo linear actuators, with stroke size of 10 cm, connecting to the platforms by universal joints. The hybrid robot created by combination of a 3DoF robot and a 6DoF robot. The six universal joints used on platform A are capable of rotating around themselves. The platforms are made by aluminium (Alloy 2024). In order to measure the applied forces, nine 6-axes Nano25 force sensors were embedded between the universal joints and clevises. A SSC-32 Servo Controller was used to control and receive force and position feedback. The developed prototype of the hybrid robot is shown in Figure 7.

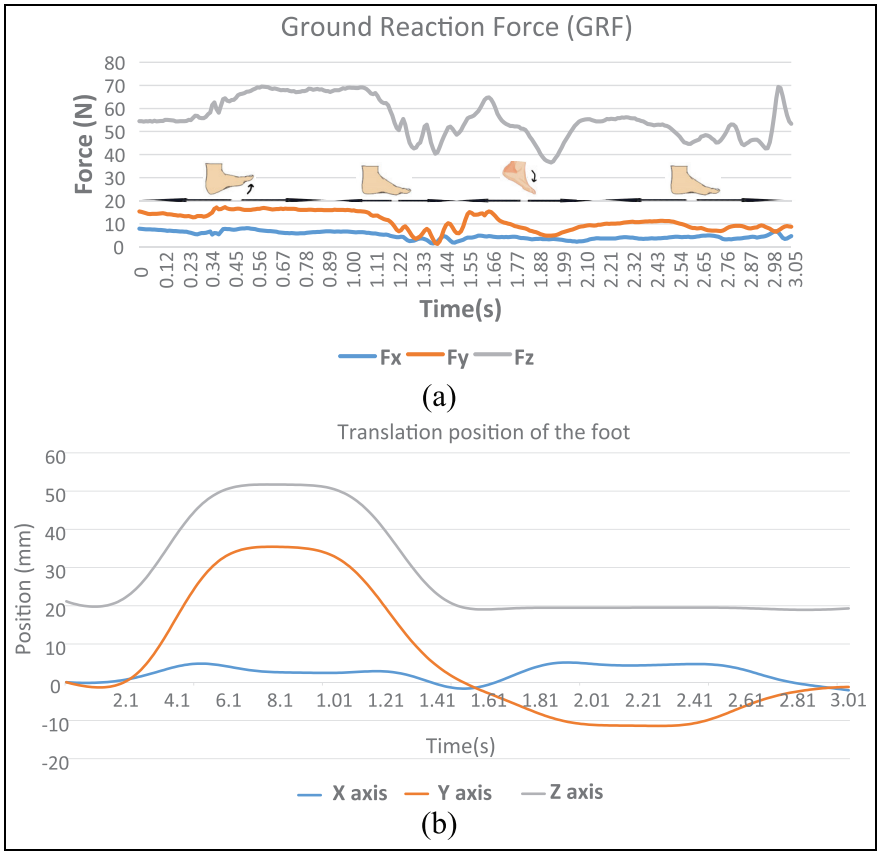

Figure 5. (a) Ground reaction forces (GRFs) in X-, Y- and Z-axes are recorded by the force plate located under the left foot, and then the corresponding values were averaged over all participants and trials. The foot moved upwards (from 0:86 s) and then moved downwards (from 0.86 s:1.49 s), then plantar flexion movement started at 1.49 s and the toe reached to its maximum height from floor at 2.11 s, and finally, foot was in the rest mode at 3.05s. (b) Position of the foot during dorsiflexion and plantar flexion.

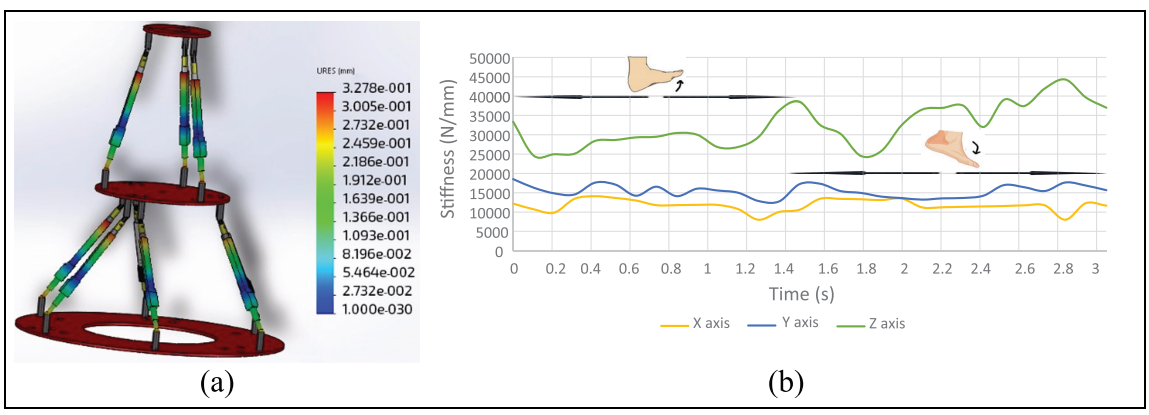

Figure 6. Translational stiffness analysis of hybrid robot in simulation: (a) deformation of actuators under load and (b) translational stiffness along X-, Y- and Z-axes during dorsiflexion and plantar flexion.

The 3D CAD model of the system, when the foot is placed on the platform, is depicted in Figure 7(b).

Protocol of experiment

The experiment was designed to determine the translational stiffness of the robot following the foot trajectory. The required actuator lengths to follow the foot trajectory were calculated by the IK and data were sent to the microcontroller to execute the motion. The calculated actuator lengths during the exercise are shown in Figure 8. Results show a higher contribution of the tripod than hexapod in tracking the foot motion by the end-effector.

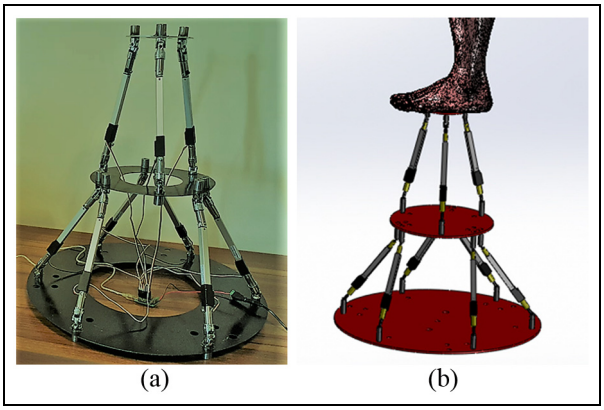

Figure 7. (a) The built 9DoF hybrid robot prototype and (b) 3D CAD model of the foot placed on the hybrid platform for ankle rehabilitation.

In order to measure the displacement of the system, the built robot was loaded with 7 kg calibration weight and the position of the robot was recorded while it was tracking the foot trajectory. Then, this value was compared with the corresponding value of unloaded robot and displacement of the robot was calculated in X-, Y- and Z-axes. The maximum ground reaction force recorded in the gait lab was 69.48 N along Z-axis, so it was decided to use similar external force in the experiment, and therefore, 7 kg weight was loaded on platform E. This experiment was repeated over 10 trials and the averaged displacement was calculated along three axes.

The applied forces on the actuators in three axes were measured by the embedded force sensors while the robot was loaded with 7 kg weigh. The Nano25 recorded Fx, Fy and Tz with 3600 Hz, and Fz, Tx, Ty with 3800 Hz. The measured forces were averaged separately for the hexapod, the tripod and in overall for the hybrid robot. The stiffness of the prototype was calculated along three axes and the results are depicted in Figure 9(a). Based on the coordinate system used in the gait lab, the X-axis was defined as a pivot axis during the exercise.

Figure 9(b) shows that the maximum stiffness error between simulation and experimental results was 5.5%, 6.6% and 4.3% in X-, Y- and Z-axes, respectively. As it is shown in Figures 6(b) and 9(a), the stiffness had a similar pattern in both simulation and experiment. In simulation, the external force was changing with respect to the time, while the external force was constant in experiment and this issue was recognised as the main source of error. It is worth mentioning that increasing the mesh size will improve the accuracy of the results in simulation.

Another case study was designed in order to investigate the stiffness behaviour of the robot when there is a constraint in Z-axis and robot moved only along X- and Y-axes. The stiffness matrix is determined as a scalar value which is attributed to the stiffness of the system. This makes the comparison easier for different configurations in the same particular position. As it is shown in Figure 10, this value was calculated when the end-effector was fixed in $Z = 50$ mm. The Z-axis is fixed to study the effect of motions on stiffness of the system. Therefore, stiffness has been replaced with Z-axis. With respect to the obtained results, the stiffness of the system is reduced when the end-effector moved along X and Y directions. The obtained results superlatively validate the experimental results in the first case study.

The results approve the high stiffness of the 9DoF hybrid parallel robot and capability of the robot to be used as an assistive robotic device for ankle

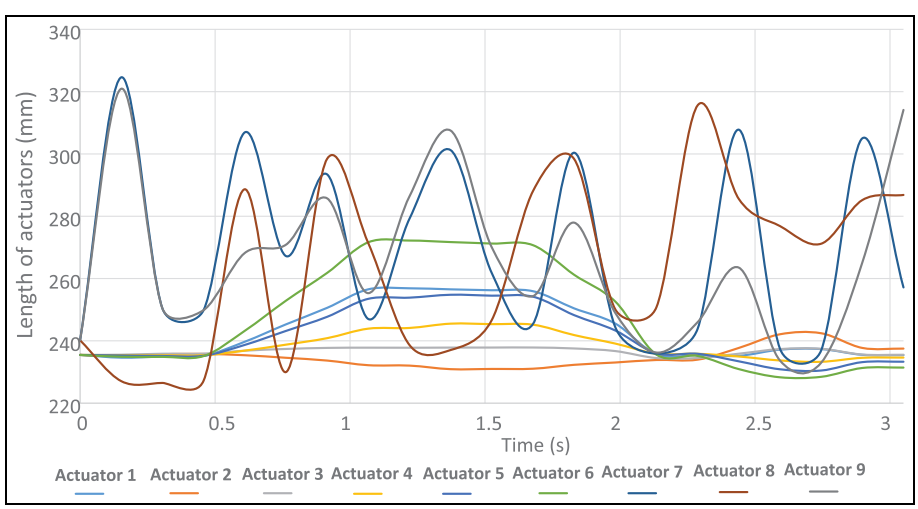

Figure 8. Length of actuators during tracking the foot motion. Actuators [1, 2, 3,..., 6] correspond to the hexapod configuration and actuators [1, 2, 3] correspond to the tripod configuration.

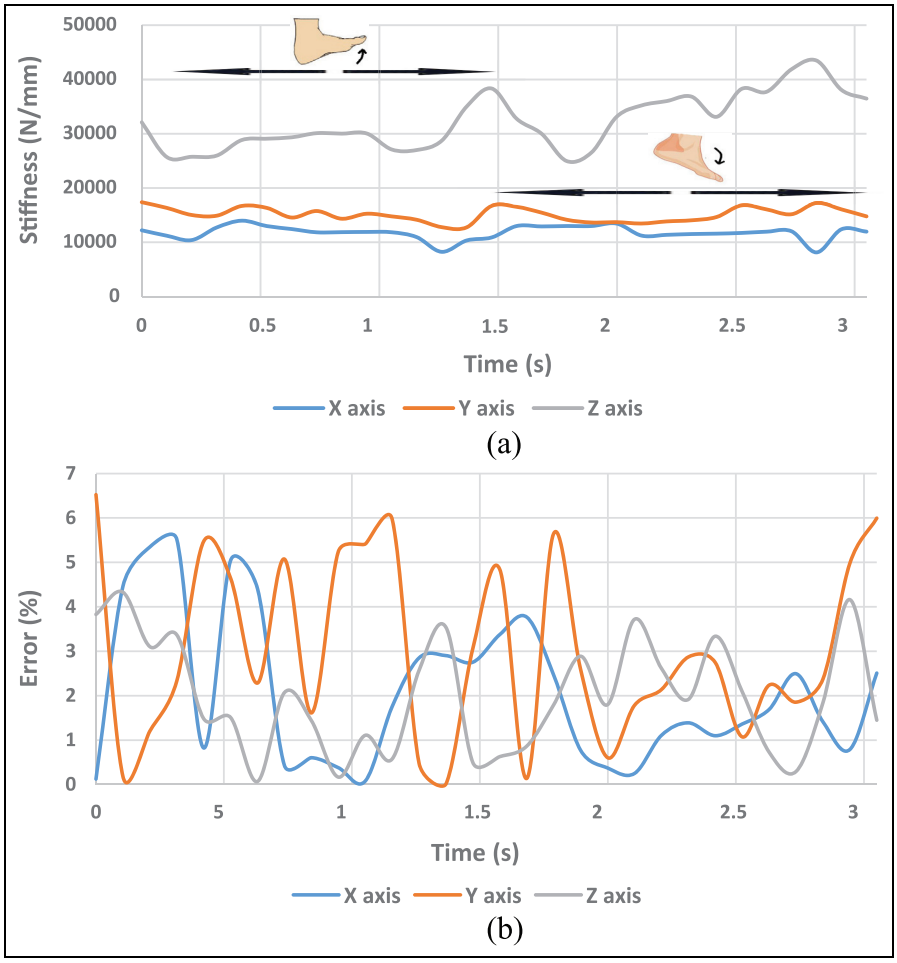

Figure 9. (a) Stiffness analysis of hybrid robot during performing dorsiflexion and plantar flexion movements and following the recorded foot trajectory and (b) Stiffness error between simulation and experimental results.

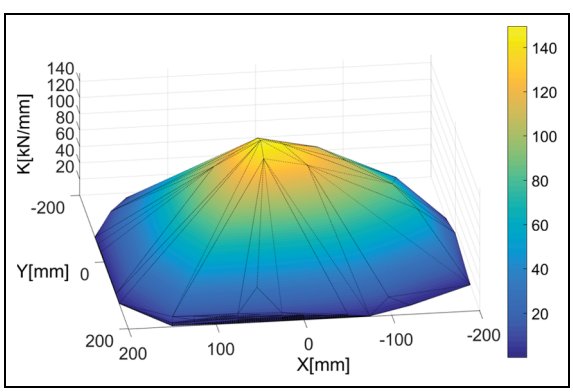

Figure 10. Stiffness of the hybrid robot when the end-effector was fixed in $Z = 50$ mm.

rehabilitation. This robot, as an alternative solution for traditional ankle rehabilitation, provides more accurate movements with respect to the range of motion of patient's joints. In future work, the stiffness of the system in more complex motions will be investigated and results will be used to optimise the design and structure of the hybrid robot.

Conclusion

This article presents a new configuration of parallel robot with increased workspace for rehabilitation of the ankle. By analysing the workspace of the robot, it was found that the robot has the capability of tracking the foot motion within the reachability range of the end-effector. Accordingly, the results show that the workspace of the hybrid parallel robot has significantly increased by 160% compared to that of the hexapod. The stiffness of the robot, during tracking the foot motion, in three single axes has been investigated in both simulation and experimentation. Translational stiffness in X-, Y- and Z-axes had the similar trend as those of calculated in experimentation. The averaged error in X-, Y- and Z-axes was 2%, 3% and 2% respectively. However, the error revealed that there are some peak error points which can be reduced by refining the

mesh points or defining more accurate contact points in the FEA. By comparing the simulation results with those of obtained from experimentation in the 1st case study, it was found that the stiffness of the end-effector increased, as robot moved downward along the Z-axis. As results depict, the designed parallel hybrid robot has the capability of performing foot rehabilitation exercise with larger workspace and higher stiffness than hexapod and tripod.

Acknowledgements

The authors would like to thank West Midlands Rehabilitation Centre (WMRC) and University College London (UCL) for their support. Alireza Rastegarpanah and Hamid Rakhodaei are identified as joint lead authors of this work.

Declaration of conflicting interests

The author(s) declared no potential conflicts of interest with respect to the research, authorship, and/or publication of this article.

Funding

The author(s) received no financial support for the research, authorship, and/or publication of this article.

ORCID iD

Alireza Rastegarpanah https://orcid.org/0000-0003-4264-6857
Alberto Borboni https://orcid.org/0000-0001-7069-1095

References

1. Hu B, Song C and Li B. Stiffness analysis of a planar 3-RPS parallel manipulator. In: *Mechatronics and robotics engineering for advanced and intelligent manufacturing*. Berlin: Springer, 2017, pp.13–28.
2. Wang Z, Chen L and Sun L. An integrated parallel micromanipulator with flexure hinges for optical fiber alignment. In: *International conference on mechatronics and automation (ICMA)*, Harbin, China, 5–8 August 2007, pp.2530–2534. New York: IEEE.
3. Simaan N and Shoham M. Stiffness synthesis of a variable geometry six-degrees-of-freedom double planar parallel robot. *Int J Robot Res* 2003; 22: 757–775.
4. Zhang Q, Li R, Li Q, et al. Analysis of the stiffness of modular reconfigurable parallel robot with four configurations. In: *International conference on intelligent robotics and applications*, Tokyo, Japan, 22–24 August 2016, pp.198–209. Cham: Springer.
5. Wang X, Ma S and Lin Q. Hybrid pose/tension control based on stiffness optimization of cable-driven parallel mechanism in wind tunnel test. In: *2nd international conference on control, automation and robotics (ICCAR)*, Hong Kong, China, 28–30 April 2016, pp.75–79. New York: IEEE.
6. Liu H, Huang T, Chetwynd DG, et al. Stiffness modeling of parallel mechanisms at limb and joint/link levels. *IEEE T Robot* 2017; 33: 734–741.
7. Zhao Y and Cheng G. Dimensional synthesis of a 3UPSPRU parallel robot. *Robotica* 2017; 35: 1–11.
8. Kumar P, Behera AK and Bandyopadhyay B. Robust finite-time tracking of Stewart platform: a super-twisting like observer-based forward kinematics solution. *IEEE T Ind Electron* 2017; 64: 3776–3785.
9. Li YW, Wang JS and Wang LP. Stiffness analysis of a Stewart platform-based parallel kinematic machine. In: *IEEE international conference on robotics and automation*, Washington, DC, 11–15 May 2002, vol. 4, pp.3672–3677. New York: IEEE.
10. Zhang D, Patel S, Gao Z, et al. Stiffness control for a 3-DOF parallel robot based machine tools. In: *International conference on information and automation*, Changsha, China, 20–23 June 2008, pp.1085–1090. New York: IEEE.
11. Masouleh MT, Saadatzi MH, Gosselin C, et al. A geometric constructive approach for the workspace analysis of symmetrical 5-PRUR parallel mechanisms (3T2R). In: *International design engineering technical conferences*, Montreal, QC, Canada, 15–18 August 2010, pp.1335–1344. New York: ASME.
12. Pisla D, Gherman B, Vaida C, et al. An active hybrid parallel robot for minimally invasive surgery. *Robot Com-Int Manuf* 2013; 29: 203–221.
13. Huang T, Wang P, Zhao X, et al. Design of a 4-DOF hybrid PKM module for large structural component assembly. *CIRP Ann: Manuf Techn* 2010; 59: 159–162.
14. Pessi P, Wu H, Handroos H, et al. Accuracy analysis of hybrid parallel robot for the assembling of ITER. *Fusion Eng Des* 2009; 84: 1964–1968.
15. Rakhodaei H, Saadat M and Rastegarpanah A. Motion simulation of a hybrid parallel robot for ankle rehabilitation. In: *12th biennial conference on engineering systems design and analysis*, Copenhagen, 25–27 July 2014, pp.V003T17A008. New York: ASME.
16. Hu B, Lu Y, Tan Q, et al. Analysis of stiffness and elastic deformation of a 2(SP + SPR + SPU) serial–parallel manipulator. *Robot Com-Int Manuf* 2011; 27: 418–425.
17. Zhao W, Li B and Hu Y. Stiffness analysis of a hybrid manipulator applied to a multi-dimensional vibration isolator. In: *International conference on mechatronics and automation (ICMA)*, Chengdu, China, 5–8 August 2012, pp.1874–1879. New York: IEEE.
18. Rastegarpanah A and Saadat M. Lower limb rehabilitation using patient data. *Appl Bionics Biomech* 2016; 2016: 2653915.
19. Meng W, Xie SQ, Liu Q, et al. Robust iterative feedback tuning control of a compliant rehabilitation robot for repetitive ankle training. *IEEE/ASME T Mechatron* 2017; 22: 173–184.
20. Lu Y, Hu B and Yu J. Analyses of the stiffness and elastic deformation of a 2(3-SPR) serial-parallel manipulator. *Proc IMechE, Part K: J Multi-body Dynamics* 2009; 223: 189–198.